



1 **Impact of the COVID-19 pandemic on the observed vertical distributions of**
2 **PM_{2.5}, NO_x, and O₃ from a tower in the Pearl River Delta**

3 Lei Li^{a, b, c}, Chao Lu^d, Pak-Wai Chan^e, Zi-Juan Lan^f, Wen-Hai Zhang^g, Hong-Long Yang^d and Hai-Chao Wang^{a, b, c*}

4 a School of Atmospheric Sciences, Sun Yat-Sen University, Zhuhai, 519082, PR China

5 b Guangdong Provincial Observation and Research Station for Climate Environment and Air Quality Change in the
6 Pearl River Estuary, Zhuhai, 519082, China

7 c Key Laboratory of Tropical Atmosphere-Ocean System (Sun Yat-sen University), Ministry of Education, Zhuhai,
8 519082, China

9 d Shenzhen National Climate Observatory, Meteorological Bureau of Shenzhen Municipality, Shenzhen, 518040,
10 PR China

11 e Hong Kong Observatory, 999077, Hong Kong

12 f Shenzhen Research Academy of Environmental Sciences, Shenzhen, 518001, PR China

13 g Shenzhen Academy of Severe Storms Science, Shenzhen, 518057, PR China

14 Corresponding author: wanghch27@mail.sysu.edu.cn

15

16 **Abstract.** The outbreak of the 2019 novel coronavirus (COVID-19) has brought tremendous impact and influence
17 on human health and social economy around the world. The lockdown implemented in China, starting on 23
18 January 2020, led to large reductions in human activities and the associated emissions. Sharp declines in primary
19 pollution provided a unique chance to examine the relationships between anthropogenic emissions and air quality.
20 Here, we report measurements of air pollutants and meteorological parameters at different heights on a tall tower in
21 the Pearl River Delta, China, to investigate the response of the vertical scales of pollutants to reductions in human
22 activities. Compared to the pre-lockdown period (starting from 16 December 2019), the observations showed that



23 surface layer NO_x , $\text{PM}_{2.5}$ and mean values of the daily maximum 8 h average O_3 (MDA8O_3) had significant
24 reductions of 76.8%, 49.4%, and 18.6% respectively, but the average O_3 increased (9.7%) during lockdown period.
25 The vertical profiles of NO_x and O_3 changed during the lockdown period, but not those of $\text{PM}_{2.5}$. The correlation
26 between $\text{PM}_{2.5}$ and O_3 was statistically significant, but not that between $\text{PM}_{2.5}$ and NO_x for data collected at four
27 different heights during the lockdown period. The significance of these correlations was the opposite during the
28 pre-lockdown period, indicating that the main composition of $\text{PM}_{2.5}$ has changed dramatically since the lockdown,
29 which is transited from primary aerosol dominating or nitrate dominating (affected by NO_x) before lockdown to
30 secondary organic aerosol dominant dominating (affected by O_3) during the lockdown. We find weaker diurnal
31 variation of O_3 during the lockdown period is similar to the case at background regions. O_3 concentrations were not
32 sensitive to NO_x concentrations during lockdown, which implies that O_3 levels during the lockdown are more
33 representative of the regional background, for which anthropogenic emissions are low and photochemical
34 formation is not a significant ozone source. This evidence suggests that significant reductions of anthropogenic
35 emissions are effective in simultaneous mitigation of $\text{PM}_{2.5}$ and O_3 levels.

36 Keywords: COVID-19 induced Lockdown, $\text{PM}_{2.5}$, NO_x , O_3 , Tower Observation

37

38 1. Introduction

39 The coronavirus disease 2019 (COVID-19) pandemic has completely changed the world and caused great
40 losses of life globally. At present, over 200 countries and regions have been affected by the pandemic, and the
41 numbers of infections and deaths caused by severe acute respiratory syndrome coronavirus 2 (SARS-CoV-2) and its
42 variants are still rising (Wang et al., 2020). Many countries have chosen to implement lockdowns to bring the
43 pandemic under control; that is, to cut off the spread of SARS-CoV-2 by reducing gatherings and maintaining
44 social distancing among individuals. These measures have generally reduced human activity, decreasing or



45 completely halting manufacturing work and the movement of people. Although the lockdowns have had devastating
46 socioeconomic impacts, recent studies have shown them to be beneficial for the environment (Chakraborty and
47 Maity, 2020).

48 The reduction in human activities due to the pandemic has greatly decreased the emission of primary
49 pollutants. This, in turn, has caused significant impacts on regional air quality (Xing et al., 2020; Salma et al., 2020;
50 Wang et al., 2021; Kim et al., 2021) and even climate (Gettelman et al., 2021), albeit differing from region to
51 region. In South East Asia, the lockdown has led to a notable decrease in the aerosol optical depth over the region
52 and in pollution outflow over the oceanic areas, while a significant decrease (27%–30%) in tropospheric nitrogen
53 dioxide (NO₂) levels has been observed over territories not affected by seasonal biomass burning (Kanniah et al.,
54 2020). Srivastava (2020) noted that the aerosol optical depth had been reduced by up to 50% over the
55 Indo-Gangetic Plain during the lockdown period. In Italy, urban road traffic decreased by 48%–60% on average
56 during the country's periods of implemented lockdowns, which greatly decreased the concentrations of NO₂ and
57 particulate matter with aerodynamic diameter less than 10 µm (PM₁₀) and less than 2.5 µm (PM_{2.5}) (Gualtieri et al.,
58 2020). Rodríguez-Urrego & Rodríguez-Urrego (2020) found that the average PM_{2.5} concentration of the 50 most
59 polluted capital cities in the world had decreased by 12% on average. By analysing the emissions data of 28 cities
60 in the USA during its first round of lockdowns (15 March 2020 to 25 April 2020), it was found that 2 out of 3 cities
61 showed greatly reduced NO₂ and carbon monoxide (CO) concentrations (with decreases up to 49% and 37%,
62 respectively) compared with the 2017–2019 historical baseline and pre-lockdown levels. These decreases in NO₂
63 and CO concentrations also increased in proportion to the local population density. However, the PM_{2.5} and PM₁₀
64 concentrations only decreased significantly in north-eastern USA, California, and Nevada, which also recorded the
65 largest decreases in NO₂ concentrations (Rodríguez-Urrego & Rodríguez-Urrego, 2020).

66 China was the first country in the world to report SARS-CoV-2 infections to the World Health Organization.



67 The atmospheric environment of China was also significantly affected by the lockdown measures taken during the
68 pandemic, with some studies showing the atmospheric NO_2 concentrations to have been greatly reduced. These
69 reductions first occurred in Wuhan before spreading to the rest of China (Wang and Su, 2020). The Pearl River
70 Delta (PRD) is one of the most important economic zones in China and is also one of the most rapidly urbanising
71 regions in the world. The intensity of human activity in this region is also amongst the highest worldwide (Li et al.,
72 2021). The PRD was once severely affected by air pollution, which manifested as increasingly frequent haze
73 weather and rising PM concentrations. Because of the optimisation of industrial structures and implementation of
74 increasingly stringent pollution control measures, the air quality over the PRD had already been improved
75 significantly over the past decade (Zhang et al., 2015). Nonetheless, because the PRD contains immense
76 transportation networks and a dense distribution of factories, it has been difficult to stamp out pollutant emissions
77 completely. Therefore, the nitric oxide (NO_x), $\text{PM}_{2.5}$, and ozone (O_3) concentrations in the PRD often spike because
78 of unfavourable weather conditions (Li et al., 2020). The pandemic lockdowns have greatly reduced the intensity of
79 human activities in the PRD in a very short time, which has created a rare opportunity for the study of air pollution
80 mechanisms in the area.

81 Ever since the advent of the COVID-19 pandemic, numerous scholars have used this unique window of
82 opportunity to gain important insights into the mechanisms of air pollution. However, most of these studies were
83 based on ground-level data or space-based measurements of atmospheric column concentrations. By contrast, there
84 are no reports about the vertical distribution of air pollutants during the COVID-19 pandemic period. The vertical
85 distribution of air pollutants is a crucial piece of the puzzle for understanding how air pollution events are formed.
86 Meteorological towers are by far the most useful platforms for studies about the vertical distribution of near-surface
87 pollutants. Unlike tethered balloons or drones, meteorological platforms can be used to obtain continuous and
88 stable measurements over a long period of time. Numerous such studies have previously been performed using the



89 325-m-tall meteorological tower in Beijing (Meng et al., 2008; Sun et al., 2010; Sun et al., 2013) and the 300-m-tall
90 tower in Boulder, USA (Brown et al., 2013).

91 The PRD has one meteorological tower, the Shenzhen Meteorological Gradient Tower (SZMGT). The
92 monitoring equipment on this tower can be used to measure several air quality factors, including $\text{PM}_{2.5}$, NO_x , and
93 O_3 concentrations. Li et al. (2020) had analysed the vertical distribution of pollutants in the PRD during the peak
94 pollution season, based on air quality data and meteorological data obtained at the SZMGT from December 2017.
95 This provided useful insights about the vertical structure of air pollutant distribution in the PRD. Shenzhen is a very
96 developed city with active human activities (Li et al., 2015) and is facing the problem of air quality (Yang et al.,
97 2020). As the beginning of the COVID-19 pandemic coincided with the peak pollution season of the PRD, data on
98 the vertical distribution of pollutants recorded by the SZMGT during this period are invaluable for revealing how a
99 decrease in human activity may affect pollutant concentrations.

100

101 2. Data and Methods

102 The observational data, from 16 December 2019 to 15 February 2020, used in this study were from a
103 meteorological observation base on the east side of the Pearl River estuary; namely, the Shiyan Meteorological
104 Observation Base (hereinafter Shiyan Base), managed by the Shenzhen National Climate Observatory (Fig. 1a).
105 The base, which lies approximately 10 km from the coastline, is in the woodland area surrounding a reservoir.
106 Because the reservoir is an important source of drinking water for the population of Shenzhen, the environment
107 within 1 km around the SZMGT is protected by law and is rarely disturbed by human activity, ensuring that the
108 underlying surface will remain natural for a long time.

109 The entire area of Shenzhen is located within the subtropical monsoon climate zone. The dominant wind
110 direction in summer is south, and the airflow brings clean air from the sea to the base. In winter, the dominant wind



direction changes to a northerly one, and the airflow carries pollutants from the inland of the PRD to the base (Li et al., 2020). The peak of the COVID-19 pandemic occurred mainly in winter, a period when the meteorological conditions are generally unfavourable to the atmospheric environment of Shenzhen.

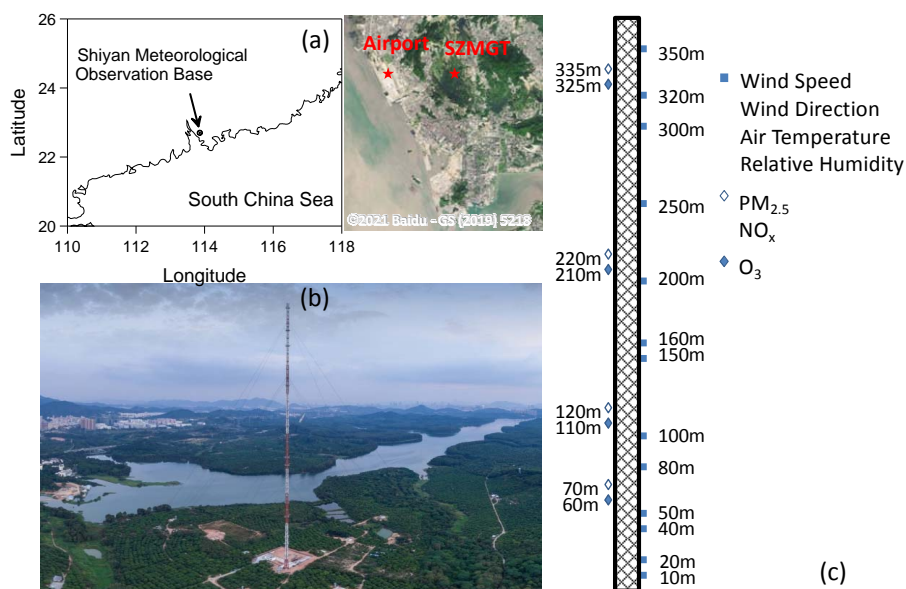


Fig. 1. Location of the Shiyan Meteorological Observation Base and Shenzhen meteorological gradient tower (SZMGT): (a) Location of the Shiyan Meteorological Observation Base; (b) Aerial view of the meteorological tower; (c) Layout of the air quality and meteorological observation on the tower.

The SZMGT, which is 365 m tall (Fig. 1b), has 13 layers of meteorological observation platforms, starting from 10 m up to 350 m (Fig. 1c). Four of those layers (i.e. at 60–70, 110–120, 210–220, and 325–335 m, respectively) are atmospheric environmental observation platforms (Fig. 1c). The distance from the SZMGT to the nearest built-up area is approximately 1 km. At 800 m north-east of the Shiyan Base, there is a busy highway from which pollutants emitted by the vehicles passing through could influence the observational data on the tower. There is also an airport located approximately 10 km west of the base which serves an estimated 356,000 flights in a



125 normal year. Thus, the airplanes taking off and landing at the airport also potentially influence the pollutant
126 concentration data recorded by the SZMGT (Li et al., 2020). An additional atmospheric environmental observation
127 station lies at the bottom of the SZMGT. Because this station is located on the ground, the height of its sampling
128 port is lower than that of the surrounding forest top.

129 The meteorological data used in the current study were collected at all 13 platform heights, as shown in Fig. 1c.
130 The environmental data were collected at the heights of 110–120, 210–220, and 325–335 m. The data at the height
131 of 60–70 m was not included in the analysis owing to the occurrence of equipment failure during the pandemic.
132 Data from the atmospheric environmental observation station at the bottom of the SZMGT were also used in the
133 current study.

134 The following are the equipment used at the SZMGT for sensing wind, temperature and humidity, and
135 visibility, respectively: the Vaisala WMT700 Ultrasonic Wind Sensor, Vaisala HMP155 Humidity and Temperature
136 Probe, and Vaisala PWD Present Weather Visibility Sensor. $\text{PM}_{2.5}$ concentration data are collected by Thermo
137 Scientific™ 5030i Sharp Particulate Monitoring equipment, NO_x by the Thermo Scientific™ 42i Gas Analyzer, and
138 O_3 by the Thermo Scientific™ 49i Gas Analyzer. The data from the various instruments were downloaded at a
139 frequency of once every 5 minutes. Arithmetic averaging of the data was performed for all the elements, except for
140 the wind direction, to obtain hourly average data. The daily average data by arithmetic averaging were obtained
141 using the hourly average data over 24 hours. For determination of the wind direction, representative values were
142 obtained by calculating the highest wind frequency by the hour and by the day.

143

144 3. Results and Discussion

145 3.1 Change of Pollutants Concentrations and Meteorological Elements

146 Fig. 2 shows the daily mean concentrations of $\text{PM}_{2.5}$, O_3 , and NO_x observed at Shiyan Base in Shenzhen from



147 16 December 2019 to 15 February 2020, as well as the daily mean relative humidity (RH), daily mean temperature,
148 daily mean wind speed, and daily dominant wind direction of this period. Two key dates have been marked with
149 blue dotted lines on the $\text{PM}_{2.5}$, O_3 , and NO_x graphs: 15 January 2020 and 23 January 2020. The first case of
150 COVID-19 in Shenzhen was reported by local news outlets on 15 January 2020. The Shenzhen government reacted
151 very quickly to this news, despite the low number of patients with COVID-19 in the area at the time. The news was
152 immediately published on the official Shenzhen government website and social restriction measures were
153 implemented. On the advice of medical experts, a lockdown was imposed on Wuhan on January 23rd. The
154 Guangdong province, where Shenzhen is located, also activated its top-level emergency response on this day, and
155 all residents in Shenzhen and her neighbouring cities were instructed not to leave their homes unless necessary.
156 Therefore, after news about the COVID-19 pandemic first appeared on January 15th, the intensity of human
157 activity in Shenzhen (both manufacturing and traffic) began to decrease. By January 23rd, Shenzhen was virtually
158 shut down because of the strengthening of activity restrictions. Other than the most vitally important logistics
159 chains, very little traffic remained on the streets. Owing to a lack of data, it has not been possible to quantitatively
160 estimate the degree to which human activity decreased in Shenzhen during this period. Nonetheless, air traffic at
161 the airport west of Shiyan Base could provide some indication of the scale. In news reports, it was mentioned that
162 the number of passengers at the airport had decreased by as much as 79.49% in February 2020. Since February
163 usually coincides with the Spring Festival (Chinese New Year), this decrease in passenger volume is enough to
164 describe the magnitude by which human activity decreased in this region.

165 As shown in Figs. 2a and 2c, the daily mean concentrations of $\text{PM}_{2.5}$ and NO_x closely tracked the
166 lockdown-mediated change in human activity. Since there were no cases of COVID-19 in Shenzhen before 15
167 January 2020, the local government did not impose any restrictions during the period between December 16th, 2019
168 and January 15th, 2020 and the pollutant concentrations remained high. After the first report of COVID-19 on



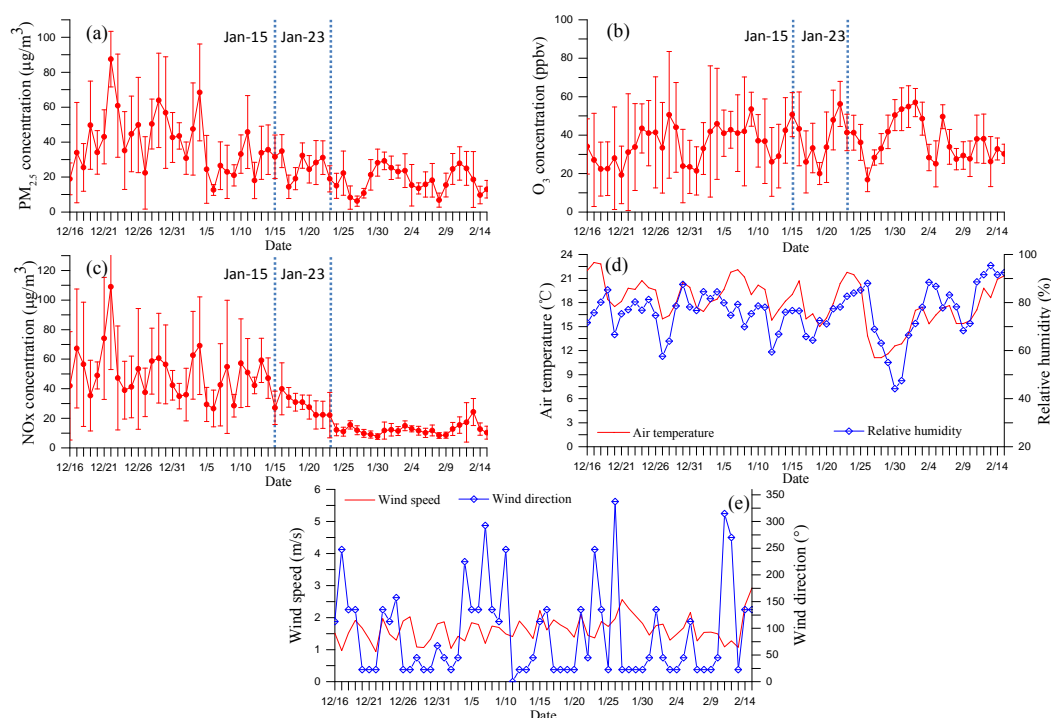
169 January 15th, many residents began to reduce the frequency of their outdoor activities owing to awareness of the
170 pandemic. Since these reductions in human activity were voluntary and not universal, the pollutant concentrations
171 only decreased slowly. However, the widespread implementation of high-level restrictions on January 23rd led to
172 drastic and sustained reductions in pollutant concentrations. The daily mean concentrations of PM_{2.5} and NO_x
173 generally remained low after January 23rd, and their ranges of variation also became significantly narrower.
174 Although all three measured pollutants were reduced by the lockdown, the change in NO_x was the most substantial.
175 This is because NO_x is primarily derived from traffic emissions, and since the decrease in human activity also
176 decreased traffic emissions, the concentration of NO_x in the atmosphere decreased instantaneously upon the
177 cessation of vehicular traffic. Meanwhile, although the daily mean concentration of O₃ did not change significantly
178 after January 23rd (Fig. 2b), the daily range of variation in its concentration (i.e. the difference between the
179 minimum and maximum O₃ concentrations in a day) did decrease significantly after this date.

180 The variations in daily mean temperature, daily mean RH, daily mean wind speed, and daily dominant wind
181 direction during the study period are shown in Figs. 2d and 2e. As evident in Fig. 2d, the RH and temperature
182 correlated strongly with each other, indicating that the dry air in the PRD comes predominantly from cold air
183 masses. During the study period, cold fronts occurred on 26–27 December 2019, 12 January 2020, and 27–30
184 January 2020. Whenever a cold air mass passes over the Shiyan Base, the daily mean temperature and RH will
185 decrease in step with each other. As evident in Fig. 2e, the daily mean wind speeds of the study period were usually
186 below 2 m/s. Additionally, the daily dominant wind direction was in the northerly direction for approximately 75%
187 of the time. The weather that was observed during the study period is common during the winters in Shenzhen,
188 indicating that no meteorological abnormalities had coincided with the study period. When we compared the
189 variations in each meteorological factor against the pollutant concentrations, only the RH and O₃ concentration
190 were found to be significantly (negatively) correlated with each other. The daily mean concentrations of PM_{2.5} and



191 NO_x were not significantly correlated with any meteorological factor during the study period.

192



193

194 **Fig. 2.** Daily variations in pollutant concentrations and related meteorological factors in the surface layer during the
 195 period of 16 December 2019 to 15 February 2020: (a) PM_{2.5} concentrations, (b) O₃ concentrations, and (c) NO_x
 196 concentrations observed at different heights; (d) Air temperature and relative humidity observed at Shiyan
 197 Meteorological Observation Base; (e) Wind speed and wind direction observed by the auto weather station at
 198 Shiyan Meteorological Observation Base. ppbv means parts per billion by volume.

199

200 Taking 23 January 2020 as a date boundary, Fig. 3 compares the average concentrations of the 3 pollutants
 201 before and during the lockdown. Fig. 3 clearly illustrates the decrease of PM_{2.5} and NO_x during the lockdown. The
 202 decrease of NO_x is much more drastic than that of PM_{2.5}. The change of O₃ is more complex than that of PM_{2.5} or



NO_x. The daily average O₃ concentration had slightly increased during the lockdown, which is consistent with the findings of other studies (Gualtieri et al., 2020). While the mean values of the daily maximum 8 h average O₃ (MDA8O₃) had significantly decreased during the lockdown. The definition of MDA8O₃ is as follows: in a natural day, take 0:00, 1:00,..., 16:00 local standard time (LST) as the starting point respectively, calculate the average concentration of O₃ for 8 consecutive hours for each starting point, and one can obtain totally 17 8-hour-average O₃ concentrations. The maximum value of all the 8-hour-average concentrations is MDA8O₃, which is generally used to assess the severity of O₃ pollution. The truth that daily O₃ concentration and MDA8O₃ had different changes means there might be quite different chemical environments related to O₃ before and during the lockdown.

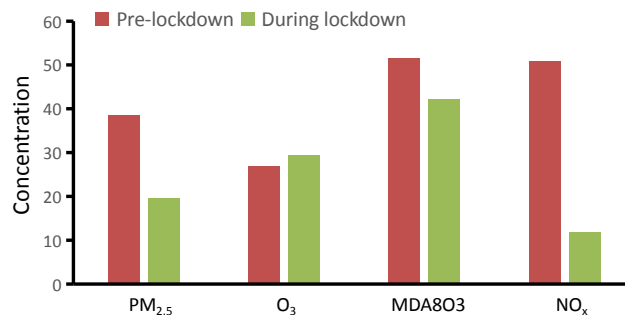


Fig. 3. Comparison of the average values of the PM_{2.5} (in µg/m³), O₃ (in ppbv), MDA8O₃ (in ppbv) and NO_x (in µg/m³) concentrations of the whole surface layer before and during the lockdown

Table 1 furtherly compares the average values of the meteorological factors and pollutant concentrations during and before the lockdown and those in the December of 2017 (Li et al., 2020). In the pre-lockdown period, the air quality in the area where the SZMGT is located had already been significantly improved compared with December 2017, which is reflected in the decrease of the average concentrations of the three pollutants.

Table 1 also provides the information on the changes of meteorological factors. In December 2017, the relative



221 humidity was lower than that in the period of the current study, which was more favorable to the photochemical
 222 reactions generating PM_{2.5} and O₃. On the other hand, the wind speed in December 2017 was much higher than that
 223 in the period of the current study, which was favorable to disperse the pollutants. Thus, it is difficult to compare the
 224 comprehensive impacts of the meteorological conditions on the pollutant's concentrations in December 2017 with
 225 those in pre-lockdown or during-lockdown period.

226

227 **Table 1.** Comparison of pollutants and meteorological elements during lockdown, before lockdown and December
 228 2017

Time period	December 2017	Before 23 Jan. 2020	After 23 Jan. 2020	Change of pre-lockdown compared with December 2017	Change during lockdown compared with before lockdown
PM _{2.5} (µg/m ³)	47.0	38.5	19.5	-18.1%	-49.4%
O ₃ (ppbv)	42.0	26.8	29.4	-36.2%	+9.7%
MDA8O ₃ (ppbv)	59.6	51.4	42.1	-13.8%	-18.6%
NO _x (µg/m ³)	54.2	50.9	11.8	-6.1%	-76.8%
Air temperature (°C)	17.1	18.9	16.5	10.5%	-12.7%
Relative humidity (%)	58.5	75.3	77.0	+28.7%	+2.3%
Wind speed (m/s)	2.2	1.6	1.8	-27.3%	+12.5%
Wind direction	NNE	NNE	NNE	—	—

229 * NNE means north-north-east. All pollutant concentrations in the table are average values for the whole surface
 230 layer recorded by the tower.

231

232 While, at least one of the possible reasons leading to the decrease of pollutants concentrations in the
 233 pre-lockdown period compared with December 2017 is quite clear, which is the strengthening of pollution emission
 234 control in Shenzhen in the past 2 years. For example, according to local news reports, in 2019 more than 1000
 235 heavy-duty diesel trucks in Shenzhen were replaced by electric trucks. In the past, the emissions of these diesel



trucks were an important source of pollution in Shenzhen.

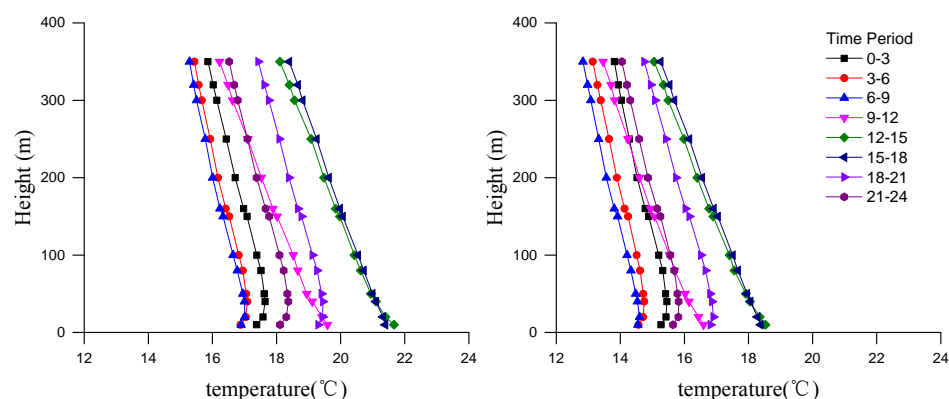


Fig. 4. Average vertical air temperature profiles recorded by the Shenzhen Meteorological Gradient Tower before and after 23 January 2020.

The changes in the meteorological factors during the lockdown compared with pre-lockdown period may largely be attributed to the intense cold air front that developed on 27–30 January 2020, which decreased the mean temperature of the lockdown period. By contrast, the RH changed very little after the lockdown was implemented. The meteorological factors that were most closely related to pollutant dispersal in the Shenzhen region were the wind speed and wind direction. Although the average wind speed increased during the lockdown, it was still weaker than that in December 2017 and never exceeded 2.0 m/s, thereby limiting any improvement in pollutant dispersion. The dominant wind direction in the pre-lockdown and lockdown periods was north-north-east, indicating that the winds in Shenzhen came mainly from the inland regions of China. In a normal year, these winds would carry a large amount of air pollution from the inland parts of the PRD and thus cause a spike in pollutant concentrations (Li et al., 2020). Therefore, it can be concluded that the meteorological conditions of the Shenzhen region were largely identical before and during the lockdown. Although an intense cold spell occurred after January 23rd and the



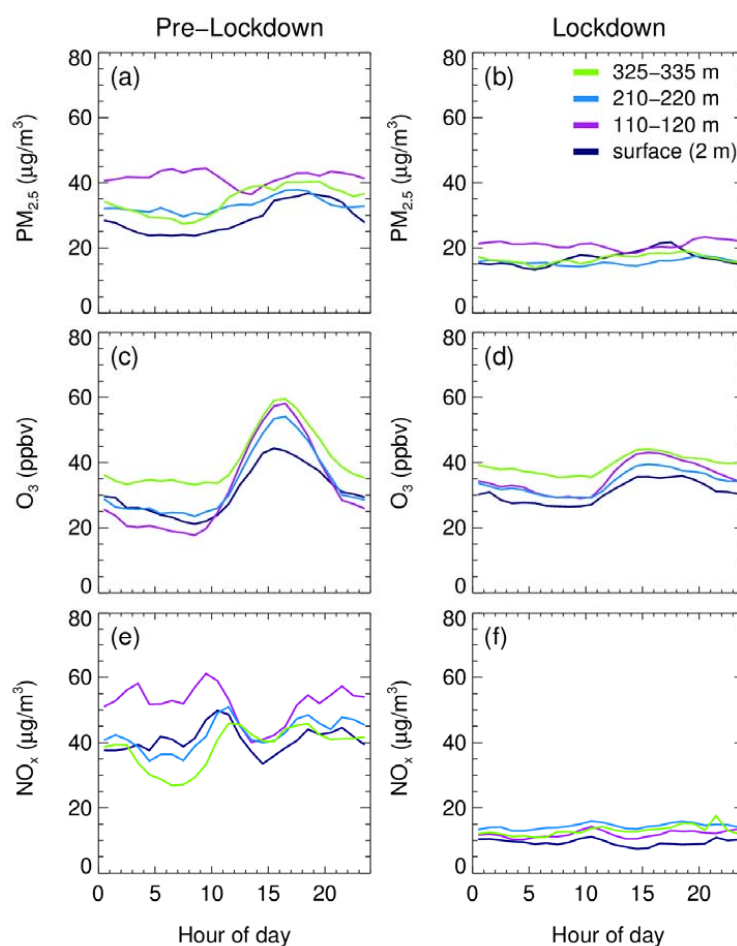
average wind speed had increased slightly, it can be learnt from the experience that these changes would not be nearly enough to cause the dramatic decreases in average $\text{PM}_{2.5}$ and NO_x concentrations recorded. Figure 4 furtherly provides the average vertical air temperature profiles recorded by SZMGT before and after 23 January 2020, from which it can be found that there is no significant difference in the stratification of air temperature before and after the outbreak of the pandemic. The data illustrated in Table 1 and Fig. 4 show that the drastic change of the pollutant concentration in the study period is almost impossible to be caused by the change of meteorological factors.

3.2 Diurnal Variations at Different Heights

Figure 5 shows the diurnal variations in $\text{PM}_{2.5}$, NO_x , and O_3 concentrations on the surface (2 m) and at three different heights of the SZMGT (120, 220, and 335 m) before and during the lockdown. The $\text{PM}_{2.5}$ time series curves in Fig. 5a are characterised by two trends: a bimodal distribution for the ground level (2 m) and 120 m curves, and a unimodal distribution for the 220 m and 335 m curves. The peaks of the bimodal curves occurred at 09:00LST and 20:00 LST, which correspond roughly to the morning and evening rush hours. The difference between the $\text{PM}_{2.5}$ curves at 0 m/120 m and that of 220 m/335 m probably reflects the uplift process of the mixing layer top in this area. During night and early morning, the height of the mixing layer top is between 120m and 220m, so the curves of the upper and lower layers are quite different. After the noon time, with the rise of the mixing layer top, the curves of all layers become to be similar. Although the $\text{PM}_{2.5}$ concentrations at 2 and 120 m followed the same qualitative trend, the values on the ground were generally lower than those at 120 m. This may have been caused by the presence of dense forests near the ground observation point (Shiyan Base), which may have obstructed the dispersal of particulate matter and thus reduced the apparent $\text{PM}_{2.5}$ concentration. The peaks of the unimodal 220 and 335 m curves occurred at 17:00–19:00 LST. Therefore, the diurnal variations in $\text{PM}_{2.5}$ concentration were different at lower and higher heights. This is consistent with the findings of Li et al. (2020),



275 whose study implied that high- and low-height $\text{PM}_{2.5}$ may have different sources. High-height $\text{PM}_{2.5}$ is formed
 276 predominantly by chemical reactions, whereas low-height $\text{PM}_{2.5}$ may be derived from multiple sources
 277 (predominantly surface-level primary emissions).



278
 279 **Fig. 5.** Diurnal variations in the pollutants observed at different heights of the meteorological tower: $\text{PM}_{2.5}$
 280 concentrations before lockdown (a) and during lockdown (b); O_3 concentrations before lockdown (c) and during
 281 lockdown (d); NO_x concentrations before lockdown (e) and during lockdown (f).

282



283 The diurnal variations in $\text{PM}_{2.5}$ concentration at 2, 120, 220, and 335 m during the COVID-19 lockdown are
284 shown in Fig. 5b. It was obvious that the $\text{PM}_{2.5}$ concentration had decreased significantly at all heights after
285 January 23rd. The 120 m curve still had the highest $\text{PM}_{2.5}$ concentration and it still retained the bimodal structure of
286 its pre-lockdown counterpart. The $\text{PM}_{2.5}$ concentrations at 220 and 335 m were still unimodal, and the peak still
287 occurred at a similar time. The biggest lockdown-mediated change in $\text{PM}_{2.5}$ concentration occurred at 2 m, where
288 the curve lost its peak in the morning and changed from a bimodal to a unimodal graph. It is likely that the morning
289 peak of the pre-lockdown curve was caused by direct emissions from nearby human activities. These emissions
290 were therefore greatly reduced by the lockdown-mediated decrease in human activity and were more easily blocked
291 by the dense forest around the ground observation point.

292 With regard to O_3 , it was evident that the diurnal variation in its concentration was unimodal and peaked at
293 approximately 15:00–16:00 LST (when photochemical O_3 formation is most active) both before and during the
294 lockdown (Figs. 5c and 5d, respectively). These diurnal variations were also qualitatively invariant with altitude;
295 that is, only the average concentration varied from one altitude to the other. However, the shape of the O_3 curve did
296 become significantly flatter during the lockdown, indicating that the range of the diurnal variations became much
297 narrower during the lockdown. The flattening of the peaks and valleys of the O_3 curve implies that the chemical
298 reactions that generate O_3 during day-time and consume O_3 during night-time became to be much inactive during
299 the lockdown. Under this condition, the O_3 concentration seemed to be determined primarily by background O_3
300 concentration (Xu et al., 2020). While, it should be noted that a flatter O_3 curve means the decrease of MDA8O_3 ,
301 which implies that the prevention of O_3 and $\text{PM}_{2.5}$ pollution can be realized at the same time theoretically.

302 In the case of NO_x , the diurnal variations in its concentration were bimodal before the lockdown (Fig. 5e). The
303 2 and 120 m curves showed a peak at 09:00 LST, which coincided with the timing of the morning rush hour. The
304 second peak, which begins at 18:00 LST and continues until 21:00 LST, was likely caused by the evening rush hour



and the night-time decrease in the altitude of the mixed layer. The first peak in both the 220 and 335 m curves lagged the first peak of the curves of lower altitude by 1 hour. However, the second peak occurred at roughly the same time in both sets of curves. Although the mean NO_x concentrations had decreased significantly during the lockdown, their diurnal variations were still bimodal (Fig. 5f). However, inter-altitude differences in NO_x concentration did become much smaller during the lockdown and the timing of the NO_x peaks at each altitude also became much closer to each other. During the lockdown, the first peak was delayed by 1 hour while the second peak occurred at 17:00–19:00 LST. The NO_x concentrations also changed in another significant way; that is, they were lower at 2 and 120 m than at 220 and 335 m. Since NO_x is a primary pollutant, its significantly lower concentrations at the low altitudes implies that near-ground chemical reactions consume it more rapidly than the high-altitude chemical reactions do.

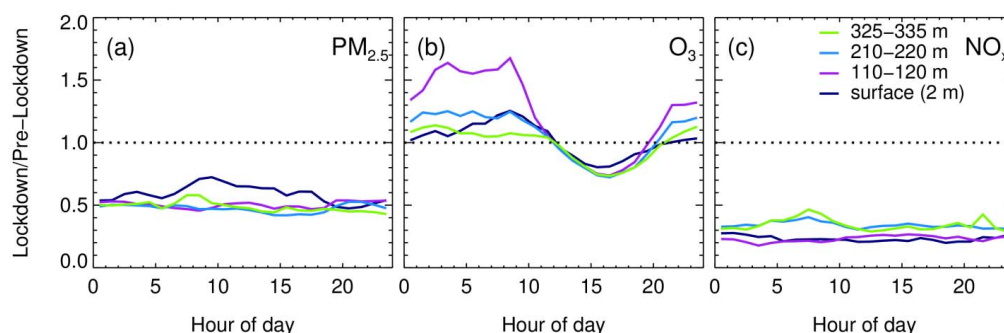


Fig. 6. Diurnal variations in the during-lockdown/pre-lockdown ratios of the pollutants observed at different heights of the meteorological tower: (a) $\text{PM}_{2.5}$; (b) O_3 and (c) NO_x .

In order to further analyze the change of the pollutants during the lockdown, the concentration ratios of the pollutants before and during the lockdown are calculated, and the diurnal variation of the ratios is illustrated in Fig. 6. The diurnal variation curves of different pollutants had different characteristics. For NO_x , the curves at different



heights were relatively consistent, which were relatively flat and maintained around 0.3, indicating that NO_x decreased significantly and evenly in the boundary layer. The curves for $\text{PM}_{2.5}$ were different. The ratio curves were relatively flat and maintained at about 0.5 all day at heights above 110 m, but there were relatively large fluctuations on the ground. The ratio on the ground increased significantly between 7:00 and 18:00 LST instead of keeping flat. Especially during 8:00 to 10:00 LST in the morning, the ratio value reached around 0.7, which showed that the decrease of ground level $\text{PM}_{2.5}$ concentration ($\sim -30\%$) during the morning “rush-hours” of lockdown was not as drastic as that of the average data of the whole boundary layer ($\sim -50\%$), though it was still difficult for the $\text{PM}_{2.5}$ generated on the ground to affect the air mass above 100 m. The fluctuation of ratio diurnal curves of O_3 was much more obvious than those of the other two pollutants. The ratios were generally greater than 1.0 in night and less than 1.0 in daytime, which showed that during lockdown, the concentration of O_3 increased in night and decreased in daytime. Especially at the height of 110-120 m, the fluctuation of the curve was more drastic, and the maximum ratio in night could reach 1.7. A possible reason leading to this phenomenon is that in the area where the SZMGT is located, the key height of night chemical reactions may be around 110-120 m. Under normal conditions, the night chemical reactions consuming O_3 in this layer may be more active than other heights. Therefore, when all emissions were weakened, the O_3 consumed by night chemical reaction was greatly reduced, and the O_3 concentration in this layer increases significantly. While this conjecture need further researches to confirm in the future.

3.3 Vertical Distribution of Pollutants

The changes in the vertical distribution of the 3 pollutants and total oxidants, Ox ($= \text{O}_3 + \text{NO}_2$), measured at 120, 220, and 335 m of the SZMGT before and during the lockdown are shown in Fig. 7. In terms of the all-day averages (Figs. 7a–7d), it was obvious that the $\text{PM}_{2.5}$, NO_x concentrations were lower at all altitudes during the lockdown. By contrast, the O_3 concentrations did not decrease significantly, but their vertical gradations did

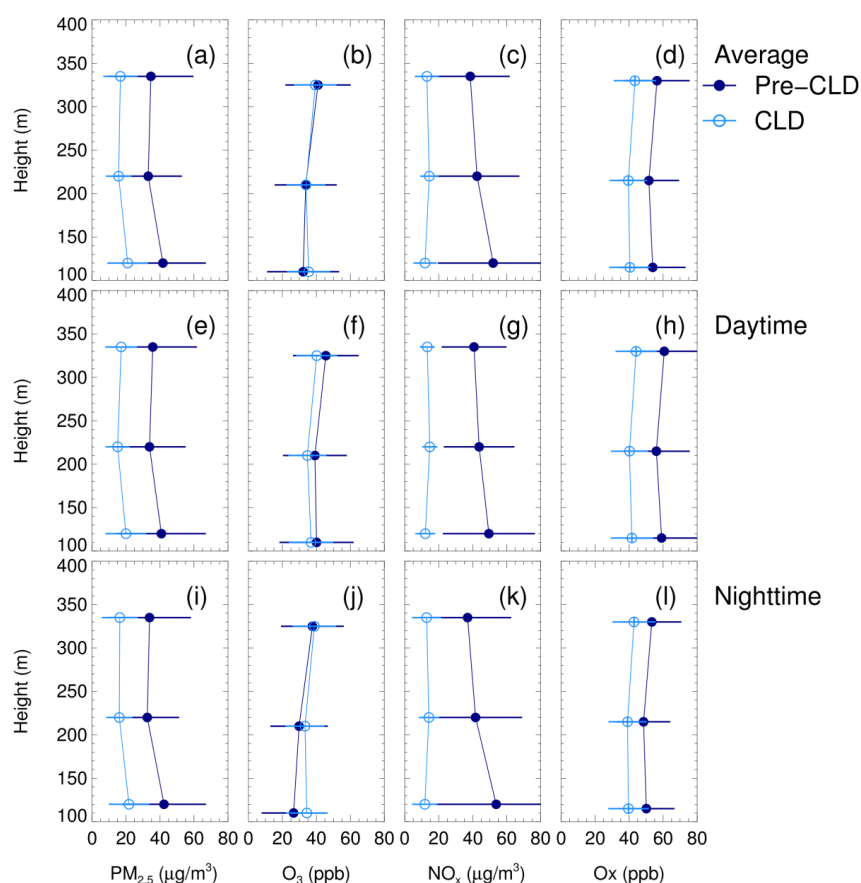


344 become less pronounced. Therefore, the O_3 concentrations became more uniform in the vertical direction during the
345 lockdown. The Ox concentrations, both on daytime and nighttime average (Figs. 7h–7i), also were generally lower
346 during the lockdown than that before the lockdown, indicating that the oxidation capacity for the whole boundary
347 layer weakened during the lockdown. We also checked the nitrate radical production rate during the nighttime,
348 which is an indicator of nighttime oxidation reactions, and showed a large decline with an average of $\sim 70\%$,
349 suggests the weaken NO_3 oxidation capacity. The decrease in nighttime oxidation is mainly attributed to cliff fall of
350 NO_x . Overall, our vertical observation showed that the atmospheric oxidation processes, including photochemistry
351 and nighttime chemistry were largely reduced due to the lockdown.

352 As shown in Fig. 7a, the $PM_{2.5}$ concentrations initially decreased with increasing altitude, before increasing
353 slightly with further increases in the altitude. This trend occurred both before and during the lockdown period. The
354 $PM_{2.5}$ concentration was the highest at the lowest observation point studied (i.e. 120 m), whereas the concentration
355 at 335 m was between those recorded at 120 and 220 m. This observation is rather interesting, as it is contrary to
356 the expectation that the $PM_{2.5}$ concentration should decrease monotonically with increasing altitude (Sun et al.
357 2010). However, this can be explained if we consider the results of previous studies about the possible sources of
358 $PM_{2.5}$ at each altitude. At the lowest height (120 m), $PM_{2.5}$ may have come from photochemical reactions and
359 primary pollution sources on the ground. At the middle level and above, $PM_{2.5}$ is formed mainly by photochemical
360 reactions (Li et al. 2020). Therefore, the efficiency of $PM_{2.5}$ generation at these heights may be affected by the
361 oxidative potential of the atmosphere. Based on the observations on the SZMGT, the O_3 concentration generally
362 increases with increasing height, and the Ox is also higher at 335 m than at 220 m. Hence, it is likely that the
363 oxidation capacity of the atmosphere is higher at the highest level, increasing the efficiency of $PM_{2.5}$ formation at
364 this altitude. Although volatile organic compound (VOC) concentrations were not measured on the SZMGT,
365 measurements in the nearby region of Taiwan have shown that these compounds also tend to increase with



366 increasing altitude, up to a peak of 300–400 m, thus providing an ample supply of reactants for photochemical
 367 reactions at high altitudes (Vo et al., 2019). At the middle level (220 m), the $\text{PM}_{2.5}$ concentration is not significantly
 368 affected by primary pollutant sources on the ground, and the $\text{PM}_{2.5}$ -forming photochemical reactions are also less
 369 efficient here than in the higher levels. Consequently, the $\text{PM}_{2.5}$ concentrations are lower in the middle level than in
 370 the high level.



371
 372 **Fig. 7.** Vertical distribution of three pollutants and Ox (= $\text{NO}_2 + \text{O}_3$) observed at the Shenzhen Meteorological
 373 Gradient Tower. Panel (a-d) show whole-day data; panel (d-h) show day-time data; and panel (i-l) show night-time
 374 data.



375 As mentioned above, the O_3 concentrations increased monotonically with increasing altitude (Fig. 7b). Even
376 during the lockdown, the average concentration of O_3 stayed high without showing any significant change.
377 Completely different from the change of O_3 , vehicular exhaust-gas emissions had plummeted to a very low level
378 during the lockdown, which is clearly evidenced in Fig. 7c. This figure shows that the NO_x concentrations had
379 decreased considerably at near-ground altitudes, especially at 120 m, where the concentration had decreased by
380 over 75% compared with pre-lockdown levels. The persistence of high O_3 concentrations during the lockdown
381 period proves the importance of VOCs for the air quality of this region once again. Actually, given the significant
382 decrease in NO_x concentrations (as much as -78.2% in the current study), the concentrations of VOCs did not seem
383 to have a same change as NO_x did. In recent studies, Qi et al (2021) reported that the decrease of VOCs in PRD
384 during the lockdown is much less than that of NO_x , and Liu et al (2021) reported that formaldehyde (HCHO)
385 abundance in the PRD area even slightly increased during the lockdown based on TROPOspheric Monitoring
386 Instrument (TROPOMI) satellite observation, which indicate that VOCs were likely to play an even more important
387 role in photochemical reactions during the lockdown period.

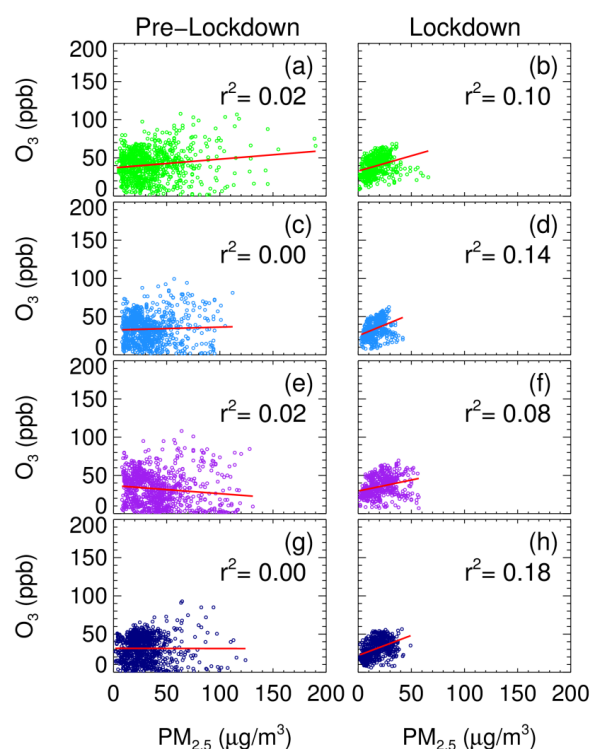
388 Figs. 7e–h and 7i–l displays the vertical distributions of pollutants and Ox during the day and night,
389 respectively. The day-time and night-time distributions of $PM_{2.5}$, NO_x and Ox were not significantly different. By
390 contrast, the vertical distribution of O_3 varied significantly between day and night. At all altitudes, the day-time O_3
391 concentrations were generally lower during the lockdown, whereas the night-time concentrations were higher. This
392 paradoxical trend can be explained by the weakening of atmospheric chemical activity during the lockdown. Since
393 the decrease in human activity during the lockdown also decreased primary pollutant emissions, the availability of
394 precursors for photochemical O_3 generation was significantly lower, resulting in decreased day-time O_3
395 concentrations. During the night, the dark chemical reactions that consume O_3 also became less active during the
396 lockdown, which resulted in significantly higher night-time O_3 concentrations at the near-surface atmosphere.



397 These changes are consistent with the diurnal variations in O_3 (Fig. 5d).

398 3.4 Correlations at Different Altitudes

399 Fig. 8 depicts scatter plots and fit lines of O_3 versus $PM_{2.5}$ at each level of the SZMGT, before and during the
 400 lockdown.



401
 402 **Fig. 8.** Scatter plots of the $PM_{2.5}$ and O_3 concentrations at different heights of the meteorological tower before and
 403 during the lockdown: (a) and (b) are for ground level; (c) and (d) are for low level; (e) and (f) are for middle level;
 404 (g) and (h) are for high level. The fit lines of the plots were produced following the instruction of Cantrell (2008).

405

406 Prior to the lockdown, the correlation between the O_3 and $PM_{2.5}$ concentrations were weak, with none of the
 407 correlation coefficients (R) passing the significance test. When performing the correlation significance test for two

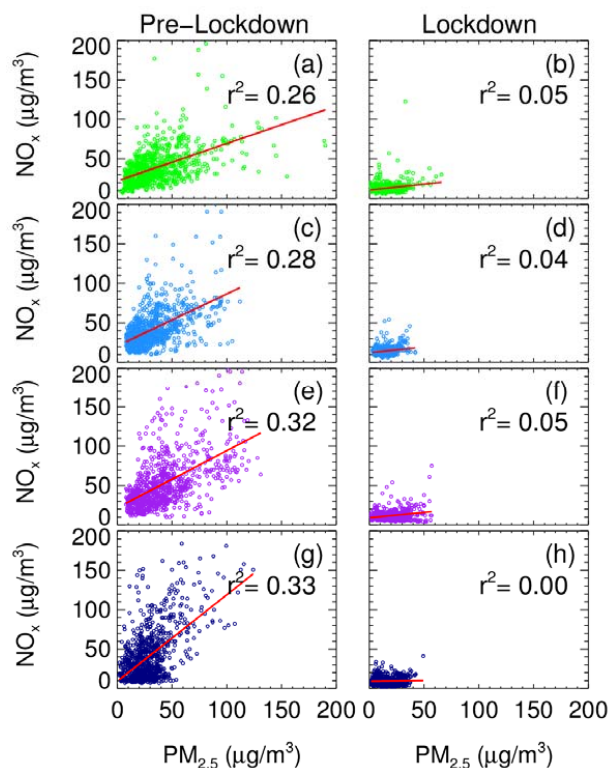


variables, namely x and y , which means two different pollutants, the Pearson correlation coefficient R was calculated. Compare R to the appropriate critical value corresponding to the $N-2$ value in a standard table, where N is size of the sample set of (x, y) pairs. If the absolute value of R is greater than the critical value, the correlation between the two variables is significant. During the lockdown, the correlation between $PM_{2.5}$ and O_3 became significantly stronger, with the R values for the 0, 120, 220, and 335 m scatter plots all being significant at the 0.1 level. It may be inferred that prior to the lockdown, $PM_{2.5}$ and O_3 did not have related sources. However, during the lockdown, both were likely to have a similar source. In the PRD region, VOCs contribute significantly to the formation of fine particles (Liu et al., 2008; Zheng et al., 2009), especially secondary organic aerosols (Huang et al., 2006; Chang et al., 2019; Zhang et al., 2019). Although the advent of the COVID-19 pandemic did result in reductions in the concentrations of NO_x , SO_2 , and other primary pollutants, the VOCs emissions might not change as dramatically as NO_x (Liu et al., 2021), which provided important precursors for both O_3 and the secondary organic aerosols during the lockdown, and strengthened the correlation between the $PM_{2.5}$ and O_3 concentrations.

Li et al. (2020) analysed the correlation coefficients of O_3 and $PM_{2.5}$ at different heights of SZMGT in December 2017, and the conclusions were different from this study. In December 2017, the correlation coefficient of O_3 and $PM_{2.5}$ increased significantly with the increase of height. They pointed out that this is because $PM_{2.5}$ is also mainly generated by photochemical reaction at high altitudes, so it has a strong correlation with O_3 . At lower heights, a considerable part of $PM_{2.5}$ is primary source and had nothing to do with photochemical reactions, so it had much weaker correlation with O_3 . While in this study, the correlation between $PM_{2.5}$ and O_3 was weak at all heights in the pre-lockdown period. The reason leading to this is mainly because that Shenzhen had conducted a large number of pollution emission control strategies in the past two years, resulting in a significant decrease in the primary pollutants. As shown in Table 1, the average concentration of $PM_{2.5}$ in the whole surface layer during the pre-lockdown period had decreased by 18.1% compared with December 2017, while the average concentration of



430 O_3 had decreased by 36.2%. The decrease of O_3 concentration in the surface layer was twice that of $\text{PM}_{2.5}$, while
 431 the primary aerosol like black carbon is not reduced, indicating that there were much fewer products of
 432 photochemical reaction and secondary aerosol formation, so that the correlation coefficient between O_3 and $\text{PM}_{2.5}$
 433 concentration was no longer high even in the higher heights. However, during the lockdown, the average
 434 concentration of $\text{PM}_{2.5}$ decreased again because the primary emission was drastically compressed. In this process,
 435 $\text{PM}_{2.5}$ formed from the primary emission became to be insignificant, and the photochemical oxidation of VOCs
 436 became to be important sources of particulate matter again. Therefore, the correlation coefficients between O_3 and
 437 $\text{PM}_{2.5}$ became to be higher than those before the lockdown.



438
 439 **Fig. 9.** Scatter plots of the $\text{PM}_{2.5}$ and NO_x concentrations at different heights of the meteorological tower before and
 440 during the lockdown: (a) and (b) are for ground level; (c) and (d) are low level; (e) and (f) are for middle level; (g)



441 and (h) are for high level.

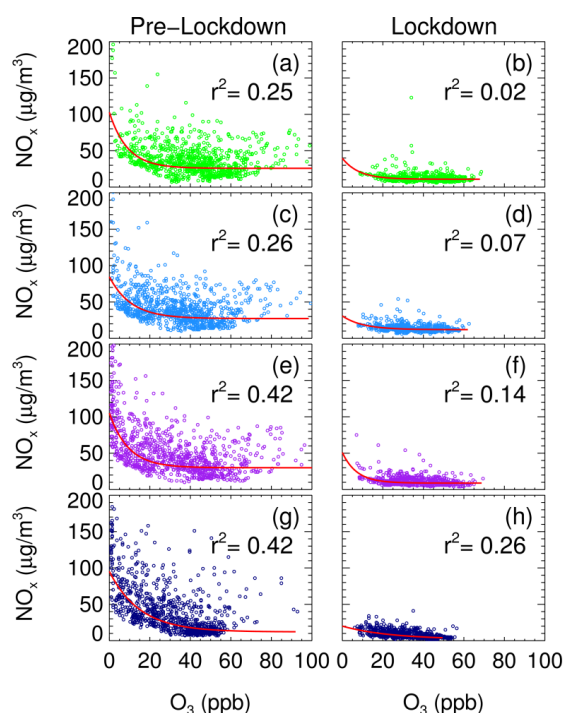
442 Fig. 9 compares the correlation between the $PM_{2.5}$ and NO_x concentrations before and during the lockdown.
443 The trend of the correlation between $PM_{2.5}$ and O_3 was the exact opposite of that between $PM_{2.5}$ and O_3 ; that is, it
444 was strong before the lockdown ($R = \sim 0.5$ at all altitudes) but much weaker after ($R = \sim 0.2$ at all altitudes).
445 Therefore, there may be significant differences between $PM_{2.5}$ sources before and during the lockdown. Owing to a
446 lack of data, it was not possible to perform a composition analysis to determine why $PM_{2.5}$ was closely correlated
447 with NO_x emissions prior to the lockdown but not during it. One possible explanation is that the primary emission
448 of $PM_{2.5}$ in the PRD is a large part before the lockdown, since NO_x can be treated as an indicator of anthropogenic
449 emission, and primary emission of $PM_{2.5}$ decreased significantly during the lockdown. The other possible
450 explanation is that the nitrate content of $PM_{2.5}$ in the PRD decreased significantly during the lockdown, given that it
451 has been previously found that nitrate accounts for a large percentage of $PM_{2.5}$ before the year of 2020 (Yang et al.,
452 2020).

453 Fig. 10 displays the correlation between the O_3 and NO_x concentrations before and during the lockdown. Prior
454 to the pandemic, O_3 and NO_x were negatively correlated with each other owing to NO_x titration. The relationship
455 between the O_3 and NO_x concentrations could be fitted with an exponential function. During the lockdown, the
456 (negative) correlation between O_3 and NO_x weakened significantly, which means that at very low NO_x
457 concentrations, variations in the concentration of this pollutant seemed to virtually have no obvious effect on the O_3
458 concentrations.

459 The comparison of scatter plots before and during the lockdown showed that $PM_{2.5}$ was poorly correlated to O_3
460 but closely correlated to NO_x before the lockdown, indicating that a large proportion of $PM_{2.5}$ might come from
461 primary emissions or nitrate aerosol. While after the implementation of the lockdown, $PM_{2.5}$ became to be closely
462 correlated to O_3 , but not to NO_x , and O_3 formation cannot attribute to the local photochemistry, indicating that



463 $\text{PM}_{2.5}$ during the lockdown might primarily be secondary pollutants (especially organic aerosols) generated from
 464 photochemical reactions.



465
 466 **Fig. 10.** Scatter plots of the O_3 and NO_x concentrations at different heights of the meteorological tower before and
 467 during the lockdown: (a) and (b) are for ground level; (c) and (d) are for low level; (e) and (f) are for middle level; (g)
 468 and (h) are for high level.

469

470 4 Conclusions and Implications

471 In this study, changes in the NO_x , O_3 , and $\text{PM}_{2.5}$ concentrations over the PRD, mediated by the local
 472 COVID-19 pandemic lockdown measures, were investigated through the analysis of their vertical distribution
 473 before and during the lockdown, using data from the Shiyan Base and SZMGT. The conclusions of this study are as
 474 follows:



475 (1) The advent of the COVID-19 pandemic forced a dramatic decrease in human activity. This greatly reduced
476 the emission of primary pollutants like NO_x , thus changing the chemical environment of the near-surface
477 atmosphere. The concentration of $\text{PM}_{2.5}$ was also reduced significantly because of the decrease in precursor
478 availability.

479 (2) The reduction in primary pollutant emissions during the COVID-19 pandemic lockdown significantly
480 decreased MDA8O_3 , while did not decrease the daily average concentration of O_3 . The diurnal curves of O_3
481 concentration were changed by the lockdown, with the day-time concentrations being lower and the night-time
482 ones being higher than the pre-pandemic concentrations at all levels of the SZMGT.

483 (3) The correlation between $\text{PM}_{2.5}$ and O_3 concentrations was insignificant before the lockdown but became
484 significantly stronger after, to the point where the correlation coefficients between $\text{PM}_{2.5}$ and O_3 were significant at
485 the 0.05 level, regardless of altitude. This indicates a strong correlation between $\text{PM}_{2.5}$ and O_3 . By contrast, the
486 correlation between $\text{PM}_{2.5}$ and NO_x was much weaker during the lockdown. Hence, the composition of $\text{PM}_{2.5}$ may
487 have changed from being predominantly from primary emissions or nitrate aerosol before the lockdown to being
488 predominantly a secondary organic aerosol thereafter. However, the validation of this hypothesis will require
489 further investigations.

490 (4) Prior to the COVID-19 pandemic, the O_3 and NO_x concentrations were significantly negatively correlated
491 with each other. This correlation virtually disappeared after the beginning of the pandemic. It may be concluded
492 that at very low NO_x concentrations, variations in its concentration have almost no effect on the O_3 concentration.

493 Overall, the advent of COVID-19 has devastated economies and societies around the world. However, the
494 dramatic reduction in human activity resulting from the lockdown measures has provided a unique opportunity for
495 researchers to study the response of the atmospheric environment to human activities. The data indicate that the
496 atmospheric chemical environment of the PRD has changed during the pandemic, leading the drastic change of



pollutants concentrations. These results have a clear indication for pollution prevention policy. In the past, quite a few environmental policy studies doubted whether it was necessary to further reduce mobile emissions, because in some areas, decreasing NO_x led to an increase of O_3 concentration. While this study shows that the continuous reduction of NO_x emission can still reduce the peak value and MDA8O_3 , although it will not further reduce the daily average value of O_3 .

Competing interests.

The authors declare that they have no conflict of interest.

Acknowledgement.

This study is supported by the Science and Technology Projects of Guangdong Province (grant number 2019B121201002), Natural Science Foundation of China (grant number 42075059, 41907185) and Guangdong Basic and Applied Basic Research Foundation (grant number 2019A1515012008)

References:

- Brown, S. S., Thornton, J. A., Keene, W. C., Pszenny, A. A. P., Sive, B. C., Dubé, W. P., Wagner, N. L., Young, C. J., Riedel, T. P., Roberts, J. M., VandenBoer, T. C., Bahreini, R., Ozturk, F., Middlebrook, A. M., Kim, S., Hubler, G., Wolfe, D.: Nitrogen, Aerosol Composition and Halogens on a Tall Tower (NACHTT): Overview of a Wintertime Air Chemistry Field Study in the Front Range Urban Corridor of Colorado. *Journal of Geophysical Research: Atmospheres*. 118: 8067-8085. 2013.
- Cantrell, C. A.: Technical note: Review of methods for linear least-squares fitting of data and application to atmospheric chemistry problems. *Atmos. Chem. Phys.*, 8, 5477-5487. 2008.



- 519 Chakraborty, I., Maity, P. COVID-19 outbreak: Migration, effects on society, global environment and prevention.
 520 Science of The Total Environment, 728: 138882. 2020.
- 521 Chang, D., Wang, Z., Guo, J., Li, T., Liang, Y., Kang, L., Xia, M., Wang, Y., Yu, C., Yun, H., Yue, D., Wang, T..
 522 Characterization of organic aerosols and their precursors in southern China during a severe haze episode in
 523 january 2017. Science of Total Environment. 691, 101–111. 2019.
- 524 Gettelman, A., Chen, C.C., Bardeen, C.G.. The climate impact of COVID-19-induced contrail changes. Atmos.
 525 Chem. Phys., 21, 9405–9416. 2021.
- 526 Gualtieri, G., Brilli, L., Carotenuto, F., V Agnoli, C., Gioli, B.. Quantifying road traffic impact on air quality in
 527 urban areas: a covid19-induced lockdown analysis in italy. Environmental Pollution, 267, 115682. 2020.
- 528 Huang, X.F., Yu, J.Z., He, L.Y., Yuan, Z., Water-soluble organic carbon and oxalate in aerosols at a coastal urban
 529 site in China: size distribution characteristics, sources, and formation mechanisms. Journal of Geophysical
 530 Research. 111: D22212. 2006.
- 531 Kanniah, K. D., Zaman, N. A. F. K., Kaskaoutis, D., Latif, M. T.. COVID-19's impact on the atmospheric
 532 environment in the SoutheastAsia region. Science of The Total Environment, 736: 139658. 2020.
- 533 Kim, H.C., Kim, S., Cohen, M., Bae, C., Lee, D., Saylor, R., Bae, M., Kim, E., Kim, B.U., Yoon, J.H., Stein, A.,
 534 Quantitative assessment of changes in surface particulate matter concentrations and precursor emissions over
 535 China during the COVID-19 pandemic and their implications for Chinese economic activity. Atmos. Chem.
 536 Phys., 21, 10065–10080. 2021.
- 537 Li, L., Chan, P.W., Wang, D., Tan, M.. Rapid urbanization effect on local climate: intercomparison of climate trends
 538 in Shenzhen and Hong Kong, 1968-2013. Climate Research. 63, 145-155. 2015.
- 539 Li, L., Chan, P.W., Deng, T., Yang, H.L., Luo, H.Y., Xia, D., He, Y.Q.. Review of advances in urban climate study
 540 in the Guangdong-Hong Kong-Macau greater bay area, China. Atmospheric Research. 261,105759. 2021.



- 541 Li, L., Lu, C., Chan, P. W., Zhang, X., Yang, H. L., Lan, Z. J., Zhang, W. H., Liu, Y. W., Pan, L., Zhang, L.. Tower
 542 observed vertical distribution of PM_{2.5}, O₃ and NO_x in the pearl river delta. *Atmospheric Environment*, 220,
 543 117083. 2020.
- 544 Liu, S., Liu, C., Hu, Q., Su, W., Yang, X., Lin, J., Zhang, C., Xing, C., Ji, X., Tan, W., Liu, H., Gao, M.. Distinct
 545 regimes of O₃ response to COVID-19 lockdown in China. *Atmosphere*. 12,184. 2021
- 546 Liu, Y., Shao, M., Lu, S., Chang, C.C., Wang, J.L., Fu, L.. Source apportionment of ambient volatile organic
 547 compounds in the Pearl River Delta, China: part II. *Atmospheric Environment*. 42, 6261–6274. 2008.
- 548 Meng, Z. Y., Ding, G. A., Xu, X. B., Xu, X. D., Yu, H. Q. Wang, S. F.. Vertical distributions of SO₂ and NO₂ in the
 549 lower atmosphere in Beijing urban areas, China. *Sci. Total Environ*. 390: 456-465. 2008.
- 550 Qi, J., Mo, Z., Yuan, B., Huang, S., Huangfu, Y., Wang, Z., Li, X., Yang, S., Wang, W., Zhao, Y., Wang, X., Wang,
 551 W., Liu, K., Shao, M.. 1.An observation approach in evaluation of ozone production to precursor changes
 552 during the COVID-19 lockdown. *Atmospheric Environment*. 262: 118618. 2021.
- 553 Rodríguez-Urrego, D., Rodríguez-Urrego, L.. Air quality during the covid-19: PM_{2.5} analysis in the 50 most
 554 polluted capital cities in the world. *Environmental Pollution*, 266: 115042. 2020.
- 555 Salma, I., Vörösmarty, M., Gyöngyösi, A.Z. Thén, W., Weidinger, T., What can we learn about urban air quality
 556 with regard to the first outbreak of the COVID-19 pandemic? A case study from central Europe. *Atmos. Chem.*
 557 *Phys.*, 20, 15725–15742. 2020.
- 558 Srivastava, A.. COVID-19 and air pollution and meteorology-an intricate relationship: A review. *Chemosphere*, 263:
 559 128297. 2021.
- 560 Sun, Y.Wang, Y., Zhang, C. Vertical Observations and Analysis of PM_{2.5}, O₃, and NO_xat Beijing and Tianjin from
 561 Towers during Summer and Autumn 2006. *Advances in Atmospheric Sciences*. 27: 123-136. 2010.
- 562 Sun, Y., Song, T., Tang, G., Wang, Y. The vertical distribution of PM_{2.5} and boundary-layer structure during



- 563 summer haze in Beijing. *Atmospheric Environment*. 74: 413-421. 2013.
- 564 Vo, T.D.H., Lin, C., Weng, C.E., Yuan, C.S., Lee, C.W., Hung, C.H., Bui, X.T., Lo, K.C., Lin, J.X.. Vertical
 565 stratification of volatile organic compounds and their photochemical product formation potential in an
 566 industrial urban area. *Journal of Environmental Management*. 217: 327–336. 2018.
- 567 Wang, C., Horby, P.W., Hayden, F.G., Gao, G.F.. A novel coronavirus outbreak of global health concern.
 568 *Lancet*. 395(10223):470-473. 2020.
- 569 Wang, S., Ma, Y., Wang, Z., Wang, L., Chi, X., Ding, A., Yao, M., Li, Y., Li, Q., Wu, M., Zhang, L., Xiao, Y., Zhang,
 570 Y., Mobile monitoring of urban air quality at high spatial resolution by low-cost sensors: impacts of
 571 COVID-19 pandemic lockdown. *Atmos. Chem. Phys.*, 21, 7199–7215. 2021.
- 572 Wang, Q., Su, M., A preliminary assessment of the impact of COVID-19 on environment: A case study of
 573 China. *Science of The Total Environment*. 138915. 2020.
- 574 Xing, J., Li, S., Jiang, Y., Wang, S., Ding, D., Dong, Z., Zhu, Y., Hao, J.. Quantifying the emission changes and
 575 associated air quality impacts during the COVID-19 pandemic on the North China Plain: a response modeling
 576 study. *Atmos. Chem. Phys.*, 20, 14347–14359. 2020.
- 577 Yang, H.L., Zhang, Y., Li, L., Chan, P.W., Lu, C., Zhang, L., Characteristics of aerosol pollution under different
 578 visibility conditions in winter in a coastal mega-city in China. *Journal Tropical Meteorology*, 26(2), 231-238.
 579 2020.
- 580 Zhang, Y.Q., Chen, D.H., Ding, X., Li, J., Zhang, T., Wang, J.Q., Cheng, Q., Jiang, H., Song, W., Ou, Y.B., Ye, P.L.,
 581 Zhang, P.L., Zhang, G., Wang, X.M.. Impact of anthropogenic emissions on biogenic secondary organic
 582 aerosol: observation in the Pearl River Delta, southern China. *Atmos. Chem. Phys.*, 19, 14403–14415. 2019.
- 583 Zhang, L., Li, L., Chan, P. W., Al., E.. Why the number of haze days in Shenzhen, China has reduced since 2005:
 584 From a perspective of industrial structure. *MAUSAM*, 1: 45-54. 2018.



585 Zheng, J., Shao, M., Che, W., Zhang, L., Zhong, L., Zhang, Y., Streets, D., Speciated VOC emission inventory and
586 spatial patterns of ozone formation potential in the Pearl River Delta, China. Environmental Science &
587 Technology. 43: 8580–8586. 2009.

588 Xu, X., Lin, W., Xu, W., Jin, J., Wang, Y., Zhang, G., Zhang, X., Ma, Z., Dong, Y., Ma, Q., Yu, D., Li, Z., Wang, D.,
589 Zhao, H.. Long-term changes of regional ozone in China: implications for human health and ecosystem
590 impacts. Elem Sci Anth, 8: 13. 2020.